

# A Crossed Molecular Beam Study of the Phenyl Radical Reaction with 1,3-Butadiene and its Deuterated Isotopologues

Xibin Gu, Fangtong Zhang, and Ralf I. Kaiser\*

Department of Chemistry, University of Hawaii at Manoa, Honolulu, Hawaii 96822

Received: October 22, 2008; Revised Manuscript Received: November 28, 2008

The reactions between the phenyl radical ( $C_6H_5$ ) and 1,3-butadiene ( $CH_2CHCHCH_2$ ) together with its D6- and D4-isotopologues were studied under single collision conditions. The scattering data suggest that the reaction proceeds via indirect scattering dynamics and is initiated by an addition of the phenyl radical to the terminal carbon atom of the 1,3-butadiene molecule to form a  $C_6H_5CH_2CHCHCH_2$  intermediate. Then, the collision complex undergoes a hydrogen atom loss through a tight exit transition state to form the 1-phenyl-1,3-butadiene product. Reactions with isotopically labeled reactants verify experimentally that the hydrogen loss originates from the terminal carbon atom of the 1,3-butadiene reactant. Our results are also compared with other phenyl radical reactions with unsaturated hydrocarbons studied earlier in our laboratory.

## 1. Introduction

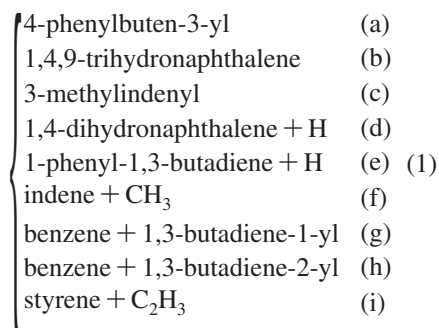
Nowadays, it is well accepted that combustion processes utilized in power generation are the major source of airborne air pollutants. The emission of these species is strongly related to lung cancer and cardiopulmonary diseases.<sup>1</sup> The predominant sources of air pollutants are nanometer-sized soot particles and polycyclic aromatic hydrocarbons (PAHs), some of which have been found to be carcinogenic (benzo[*a*]pyrene),<sup>2</sup> mutagenic,<sup>3</sup> and teratogenic. PAHs, however, are not only found in terrestrial environments but are also ubiquitous in the interstellar medium;<sup>4</sup> for instance, PAH-like species are thought to contribute to the unidentified infrared emission bands (UIBs) observed between 3 and 15  $\mu\text{m}$ .<sup>5</sup> It is also estimated that PAHs and related molecules such as their radicals, ionized PAHs, and heteroaromatic PAHs make up to 20% of the total cosmic carbon budget.<sup>6</sup>

Due to the carcinogenic character of PAHs, it is clearly imperative to minimize the formation of these molecules in combustion processes. Therefore, it is of great practical importance to gain a fundamental understanding of the underlying formation processes and also to rationalize the chemical processes responsible for the growth of soot. This will be only possible on the basis of a correct physical and chemical understanding of the combustion processes. Consequently, a significant research endeavor on PAHs and soot particles has been undertaken during the past decades. It is well accepted now that the phenyl radical ( $C_6H_5$ ) in its  $^2A_1$  electronic ground state presents one of the most crucial transient species to trigger PAH formation.<sup>7,8</sup> Chemical reaction networks concur that phenyl radical reactions with unsaturated hydrocarbon molecules such as (substituted) acetylenes, olefins, and aromatic molecules initiate the PAH synthesis. Depending on the temperature and pressure conditions, theoretical investigations coupled with kinetics studies of these reactions indicated that the intermediates either decompose back to the reactants, fragment predominantly via atomic hydrogen loss pathways, isomerize prior to their decomposition, and/or are stabilized at higher pressures if the lifetime of the intermediate is longer than the time scale

necessary to divert the internal energy of the complexes via a third-body collision.<sup>9</sup> Due to this importance, we have conducted a systematic study of the reactions of phenyl radicals with acetylene ( $C_2H_2$ ),<sup>10</sup> ethylene ( $C_2H_4$ ),<sup>11</sup> methylacetylene ( $CH_3CCH$ ),<sup>12</sup> allene ( $H_2CCCH_2$ ),<sup>12</sup> propylene ( $CH_3CHCH_2$ ),<sup>13</sup> and benzene ( $C_6H_6$ )<sup>14</sup> utilizing the crossed molecular beams approach.<sup>15</sup> These hydrocarbons serve as simple prototype molecules with triple (acetylene) and double (ethylene) bonds as well as monocyclic (benzene) aromatic species. In this paper, we expand these studies and unravel the chemical dynamics of the phenyl radical reaction with an important  $C_4H_6$  isomer, that is, 1,3-butadiene ( $H_2CCHCH_2$ ). This reaction can access the important  $C_{10}H_{10}$  potential energy surface, which also includes dihydronaphthalene. Although both reactants are important intermediates in hydrocarbon flames,<sup>16</sup> this elementary reaction of phenyl radicals with 1,3-butadiene has neither been included into models simulating the growth of PAHs nor studied under single-collision conditions to date.<sup>17–26</sup> These networks only suggest that 1,3-butadiene acts as a precursor to radicals such as  $C_2H_3$ ,<sup>27</sup>  $CH_3$ ,<sup>28</sup> and  $C_3H_3$ <sup>28</sup> and small molecules like  $C_2H_2$ <sup>29</sup> and  $C_2H_4$ <sup>29</sup> but not to more complex species like PAHs.

What is so far known on the reaction of the phenyl radical with 1,3-butadiene? Fascella et al.<sup>30</sup> investigated the reaction of the phenyl radical with 1,3-butadiene theoretically. QRRK theory was employed to estimate the overall reaction rates at temperatures between 500 and 2500 K at pressures ranging from 1 to 0.01 atm with the G2MP2 theory. This study suggested that there is no entrance barrier for the reaction between the phenyl radical and 1,3- $C_4H_6$  to form an additional intermediate of the formula  $C_{10}H_{11}$ . However, an entrance barrier of about 27  $\text{kJ mol}^{-1}$  was found for the hydrogen abstraction process to yield the 1,3- $C_4H_5$  radical plus benzene. The predicted products of the reaction are compiled in eq 1. Under single-collision conditions, the most abundant molecule over the complete temperature range of 500 – 2500 K was predicted to be 1,4-dihydronaphthalene (1d), a precursor to naphthalene in combustion flames.

\* To whom correspondence should be addressed. E-mail: ralfk@hawaii.edu.



One year later, Lin et al.<sup>31</sup> conducted an experimental study of this system at a total pressure of 40 Torr with argon as a bath gas using the cavity ring down spectroscopy. The rate constant for the phenyl radical disappearance was found to follow the relationship  $(3.16 \pm 0.29) \times 10^{12} \times \exp[-(870 \pm 30)/T] \text{ cm}^3 \text{ mol}^{-1} \text{ s}^{-1}$  over the temperature range of 298 to 450 K. Computations at the B3LYP 6-31G(d,p) level of theory suggested that at temperatures less than 1000 K, the dominant product is the initial 4-phenylbuten-3-yl (C<sub>10</sub>H<sub>11</sub>) adduct (1a). At about 1000–1400 K, 1-phenyl-1,3-butadiene (C<sub>10</sub>H<sub>10</sub>) became the main product (1e). Over 1400 K, the most important process was predicted to be the bimolecular hydrogen abstraction to form benzene (C<sub>6</sub>H<sub>6</sub>), channels 1g and 1h. The formation rates of the bicyclic species 1,4-dihydro-naphthalene (1d) were predicted to be at least one order of magnitude lower than that of the dominant channel. These conclusions are distinctly different from the results of Fascella et al.<sup>30</sup> Therefore, our crossed beam studies help to answer the question “What is the dominant product of this reaction?” under single-collision conditions.

## 2. Experimental Section

The experiments were conducted in a crossed molecular beam machine under single-collision conditions at the University of Hawaii.<sup>15</sup> Briefly, two source chambers were located inside of the scattering chamber at perpendicular geometry. One of the source chambers was used to generate the pulsed, supersonic phenyl radical beam via a modified flash pyrolytic source.<sup>32,33</sup> The nitrosobenzene (C<sub>6</sub>H<sub>5</sub>NO, Fluka 97.5%+) precursor was kept inside of a stainless steel reservoir at 283 K. Helium carrier gas was introduced into the reservoir at 4 atm to seed the nitrosobenzene precursor at fractions of less than 0.1%. The mixture was released at a backing pressure of 920 Torr via a piezoelectric pulsed valve<sup>33</sup> operated at 200 Hz and expanded through a resistively heated silicon carbide tube at a temperature of about 1200–1500 K. Under these experimental conditions, the decomposition of nitrosobenzene molecule to form the

phenyl radical and nitrogen monoxide was quantitative.<sup>34</sup> After passing a skimmer, a part of the phenyl radical beam was selected by a four-slot chopper wheel. The peak velocities and speed ratios of the segments crossing in the interaction region are listed in Table 1. The second source chamber introduced a pulsed and neat 1,3-butadiene beam (Fluka, 99.5%+) at a backing pressure of 550 Torr perpendicularly in the interaction region inside of the scattering chamber. An experiment with 1,3-butadiene-D6 (CDN, 99+D) was conducted to identify the position of hydrogen loss (does it come from the phenyl radical or from 1,3-butadiene?). Furthermore, 1,3-butadiene-1,1,4,4-D4 (CDN, 99+D) was utilized to elucidate the extent of the hydrogen versus deuterium atom loss position(s) of 1,3-butadiene, that is, from the terminal C1/C4 carbon atoms versus the C2/C3 carbon atoms.

The reactively scattering products were detected using a triply differentially pumped quadrupole mass spectrometric detector in the time-of-flight (TOF) mode, which could be rotated within the plane defined by the two supersonic beams. This device allows taking angular-resolved TOF spectra. The electron impact ionizer is operated at 80 eV with an emission current of 2 mA. By integrating the TOF spectra at distinct laboratory angles, correcting for the day-to-day intensity fluctuations of the phenyl radical beam, and normalizing to the center-of-mass angle, we obtained the laboratory angular distribution in the laboratory frame (LABORATORY), which characterized the integrated signal intensity of an ion of distinct *m/z* value versus the laboratory angle. The information on the chemical dynamics was gained by fitting these TOF spectra and the laboratory angular distribution using a forward-convolution routine.<sup>35</sup> This approach assumed an angular distribution *T*(θ) and a translational energy distribution *P*(E<sub>T</sub>) in the center-of-mass reference frame (CM), which contain all of the basic information on the reactive scattering process. TOF spectra and the laboratory angular distribution were then calculated from these center-of-mass functions. Since previous kinetics studies<sup>30</sup> of the phenyl radical reactions with 1,3-butadiene showed the absence of an entrance barrier to this reaction, we included an energy-dependent cross section,  $\sigma(E_C) \sim E_C^{-1/3}$ , with the collision energy *E<sub>C</sub>*.<sup>36</sup> Due to the low signal counts, we had to record up at least  $6 \times 10^6$  TOF spectra to obtain a reasonable signal-to-noise ratio of the reactively scattered species. This limited us to carry out the experiments with the deuterated 1,3-butadiene reactants only at the corresponding center-of-mass angles.

## 3. Results

**3.1. Laboratory Data.** In the reaction of the phenyl radical (C<sub>6</sub>H<sub>5</sub>) with 1,3-butadiene (C<sub>4</sub>H<sub>6</sub>), the reactive scattering signal was monitored at mass-to-charge ratios from *m/z* = 130 (C<sub>10</sub>H<sub>10</sub><sup>+</sup>) down to 126 (C<sub>10</sub>H<sub>6</sub><sup>+</sup>). At each angle, the TOF spectra recorded at lower *m/z* ratios showed identical pattern as those

**TABLE 1: Peak Velocities (*v<sub>P</sub>*) and Speed Ratios (*S*) of the Supersonic Beams Together with the Resulting Center-of-Mass Angles (*θ<sub>CM</sub>*) and the Corresponding Collision Energies (*E<sub>C</sub>*)<sup>a</sup>**

	<i>v<sub>P</sub></i> (ms <sup>-1</sup> )	<i>S</i>	<i>E<sub>C</sub></i> (kJ mol <sup>-1</sup> )	<i>θ<sub>CM</sub></i> (degree)
C <sub>6</sub> H <sub>5</sub> (X <sup>2</sup> A <sub>1</sub> )	2604.6 ± 19.6	4.7 ± 0.3	117.3 ± 2.2	11.9 ± 0.4
C <sub>6</sub> H <sub>5</sub> (X <sup>2</sup> A <sub>1</sub> )	2959.7 ± 60.3	5.9 ± 0.6	148.7 ± 6.3	10.5 ± 0.5
H <sub>2</sub> C=CHCH=CH <sub>2</sub> (X <sup>1</sup> A')	779.6 ± 21.8	6.9 ± 0.7		
C <sub>6</sub> H <sub>5</sub> (X <sup>2</sup> A <sub>1</sub> )	2995.4 ± 45.7	5.9 ± 0.5	161.0 ± 5.2	11.2 ± 0.4
D <sub>2</sub> C=CDCD=CD <sub>2</sub> (X <sup>1</sup> A')	760.0 ± 20.0	5.9 ± 0.9		
C <sub>6</sub> H <sub>5</sub> (X <sup>2</sup> A <sub>1</sub> )	2956.4 ± 21.5	5.5 ± 0.3	154.1 ± 2.6	11.0 ± 0.4
D <sub>2</sub> C=CHCH=CD <sub>2</sub> (X <sup>1</sup> A')	760.0 ± 20.0	5.9 ± 0.9		

<sup>a</sup> The peak velocities and corresponding speed ratios refer to those segments of the pulsed beams which were crossed in the interaction region.

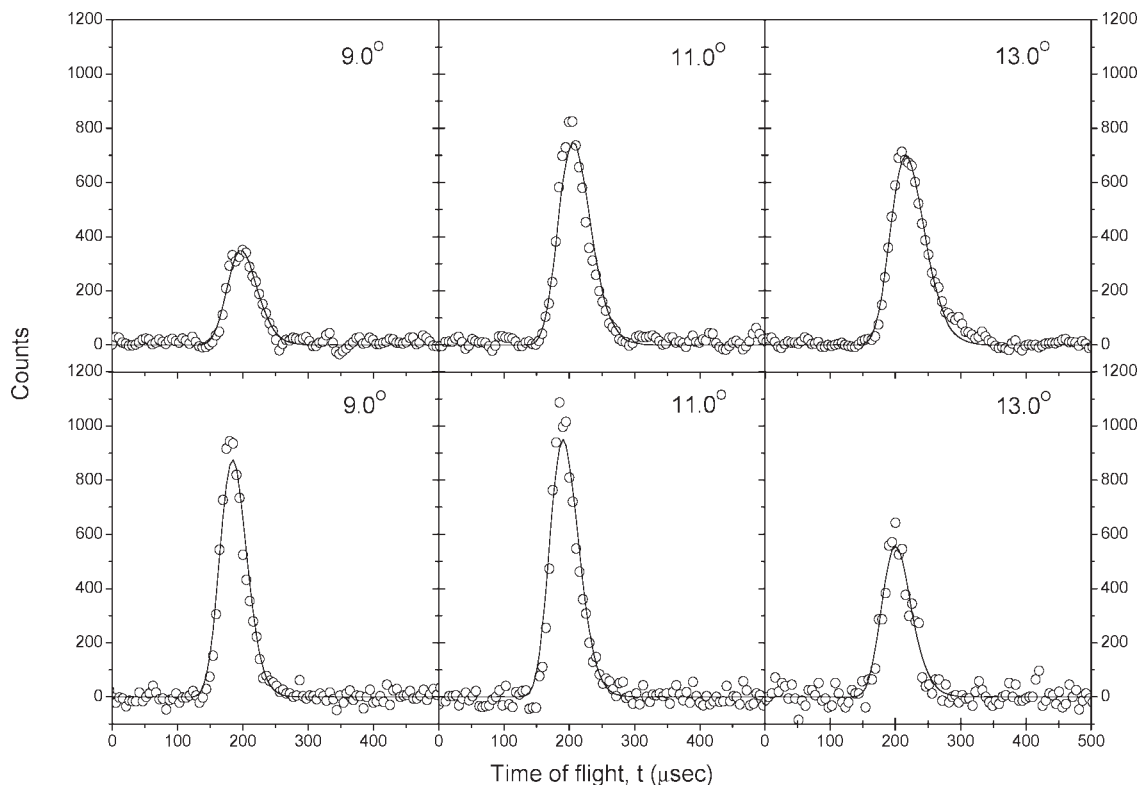
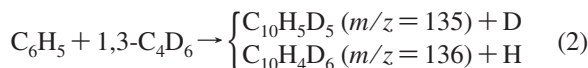


**Figure 1.** Selected time-of-flight (TOF) spectra recorded at a mass-to-charge ratio of  $m/z = 128$  ( $\text{C}_{10}\text{H}_8^+$ ), which is a fragment of the  $\text{C}_{10}\text{H}_{10}$  parent molecules, during the reaction of the phenyl radical with 1,3-butadiene at collision energies of  $117.3 \pm 2.2$  (upper row) and  $148.7 \pm 6.3 \text{ kJ mol}^{-1}$  (lower row). The open circles are the experimental data, and the solid lines are the fits.

at  $m/z = 130$  and could be fit with identical center-of-mass functions as those data taken at  $m/z = 130$ . This suggests that signals in the range of  $m/z = 129$ – $126$  originated from dissociative ionization of the parent molecule ( $\text{C}_{10}\text{H}_{10}$ ) in the electron impact ionizer of the detector. In addition, we can conclude that only the phenyl radical versus hydrogen atom exchange pathway is open within this mass range. Considering the signal-to-noise ratio and data accumulation time, we recorded all of the TOF spectra at the strongest signal ion at  $m/z = 128$  (Figure 1). Besides the atomic hydrogen loss, we also investigated the possible methyl group ( $\text{CH}_3$ ) (1f) and vinyl group ( $\text{C}_2\text{H}_3$ ) loss channels (1i). Here, we monitored ion counts at  $m/z = 116$  ( $\text{C}_9\text{H}_8^+$ ),  $115$  ( $\text{C}_9\text{H}_7^+$ ),  $104$  ( $\text{C}_8\text{H}_8^+$ ), and  $103$  ( $\text{C}_8\text{H}_7^+$ ). Nevertheless, a reactive scattering signal was observed neither from the methyl nor from the vinyl loss pathway; TOF spectra recorded at these lower masses were superimposable with those taken at  $m/z = 130$  after scaling. In contrast to the kinematically favored hydrogen atom loss channel, the potential methyl and vinyl loss channels would be more difficult to observe due to the unfavorable kinematics and also larger recoil spheres. Accounting for the data accumulation times at  $m/z = 128$  versus  $116$  and  $104$  and the signal-to-noise ratio of our experiments, we can evaluate that the upper limits of the importance of both channels are less than 10%. Due to the high background noise level at  $m/z = 78$  ( ${}^{13}\text{CC}_5\text{H}_5^+$ ) from elastically scattered reactants, the bimolecular hydrogen abstraction pathway to form benzene ( $\text{C}_6\text{H}_6$ ) was undetectable. The collected TOF spectra present the basis to derive the laboratory angular distribution of the signal recorded at  $m/z = 128$  ( $\text{C}_{10}\text{H}_8^+$ ) by integrating the TOF spectra at each angle and accounting for the data accumulation times (Figure 2). Obviously, the LABORATORY distributions are very narrow and spread only over about  $15^\circ$  in the scattering plane defined by both supersonic beams. Moreover, they are slightly forward peaked with respect to the primary beam.

To answer the question whether the hydrogen atom originated from the phenyl radical or from the 1,3-butadiene reactant, we conducted the experiments of the phenyl radical with D6-1,3-butadiene (eq 2). If a hydrogen atom elimination takes place from the phenyl group, a signal should be detected for the atomic hydrogen loss at  $m/z = 136$  ( $\text{C}_{10}\text{H}_4\text{D}_6^+$ ); if an atomic deuterium loss pathway is present (from 1,3-butadiene-D6), we should yield signal at  $m/z = 135$  ( $\text{C}_{10}\text{H}_5\text{D}_5^+$ ). In this experiment, we observed a reactive scattering signal at  $m/z = 135$ ; a very weak signal was monitored at  $m/z = 136$  at the center-of-mass angle close to  $11^\circ$ . The signal obtained at  $m/z = 136$  is superimposable on the TOF recorded at  $m/z = 135$  (Figure 3 lower) and can be attributed to  $({}^{13}\text{CC}_9\text{H}_5\text{D}_5^+)$ . Therefore, it is clear that the reaction of the phenyl radical with D6-1,3-butadiene only leads to a deuterium atom emission; consequently, in the corresponding reaction of the phenyl radical with 1,3-butadiene, the emitted hydrogen atom originated solely from the 1,3-butadiene reactant but not from the phenyl radical.



Next, we would like to collect additional information on the position of the hydrogen atom loss from the 1,3-butadiene molecule and aim to unravel to what extent the hydrogen is lost from the terminal C1/C4 carbon atoms versus the C2/C3 carbon atoms. To gain insight into this, we carried out the experiment of the phenyl radical with 1,3-butadiene-1,1,4,4-D4 (eq 3). In case of a hydrogen atom loss, signal should be detected at  $m/z = 134$  ( $\text{C}_{10}\text{H}_6\text{D}_4^+$ ); if a deuterium atom elimination takes place, we should observe ion counts at  $m/z = 133$  ( $\text{C}_{10}\text{H}_7\text{D}_3^+$ ). Note that, in principle,  $m/z = 133$  can also arise from fragmentation of  $m/z = 134$ . Within the signal-to-noise limit, we observed signal at  $m/z = 133$  (Figure 3 upper) but could not monitor any ion counts at  $m/z = 134$ . This

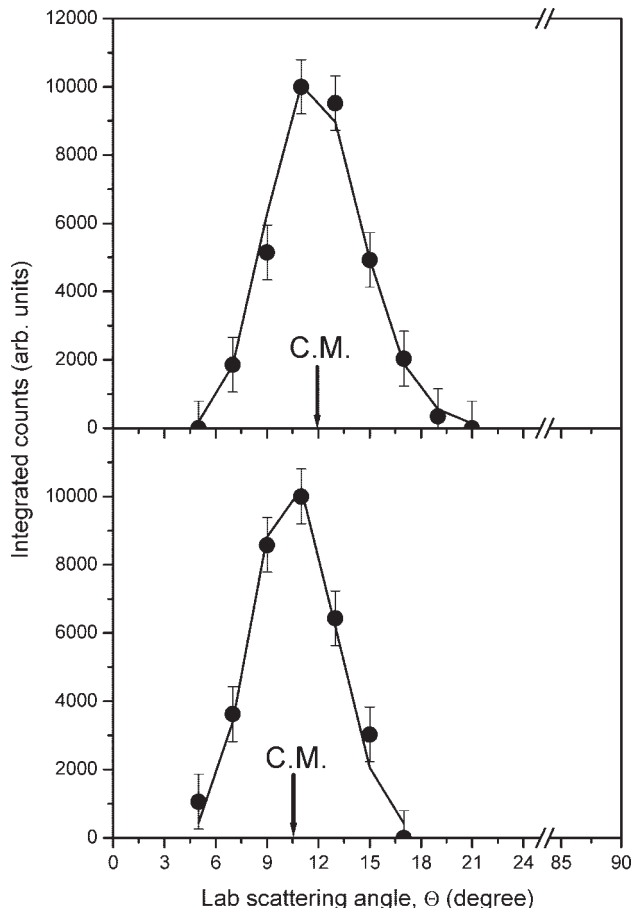
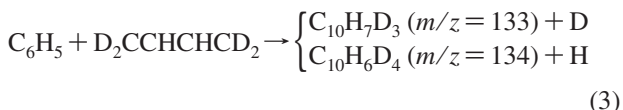


**Figure 2.** Laboratory angular distributions of ion counts recorded at  $m/z = 128$  ( $\text{C}_{10}\text{H}_8^+$ ) in the reaction of phenyl with 1,3-butadiene at collision energies of  $117.3 \pm 2.2$  (upper) and  $148.7 \pm 6.3$   $\text{kJ mol}^{-1}$  (lower). The solid circles are the experimental data, and the solid lines are the fits.

indicates that only a deuterium atom is being released from the C1/C4 positions of the D4-butadiene molecule. Consequently, in the reaction of phenyl with 1,3-butadiene, the hydrogen atom is emitted from the terminal C1/C4 carbon atom of 1,3-butadiene.



**3.2. Center-of-Mass Translational Energy,  $P(E_T)$ s, and Angular Distributions,  $T(\theta)$ s.** The TOF spectra verify the formation of a  $\text{C}_{10}\text{H}_{10}$  isomer plus a hydrogen atom in the reaction between the phenyl radical and 1,3-butadiene. Further, the studies with D4- and D6-1,3-butadiene depict explicitly that the hydrogen atom is solely released from the terminal C1/C4 positions of the 1,3-butadiene molecule. We now convert the laboratory data into the center-of-mass reference frame and discuss the resulting center-of-mass angular  $T(\theta)$  and translational energy  $P(E_T)$  distributions. At both higher and lower collision energies, a reasonable fit of the TOF data (Figure 1) and LABORATORY distributions (Figure 2) could be achieved with only a single reaction channel. The corresponding center-of-mass translation energy distributions,  $P(E_T)$ s, are shown in Figure 4 (left), which could be obtained with distributions extending to a maximum translational energy release,  $E_{T,\max}$ , of  $162.0 \pm 20.0$  and  $200.0 \pm 20.0$   $\text{kJ mol}^{-1}$  at collision energies of  $117.3 \pm 2.2$  and  $148.7 \pm 6.3$   $\text{kJ mol}^{-1}$ , respectively. The

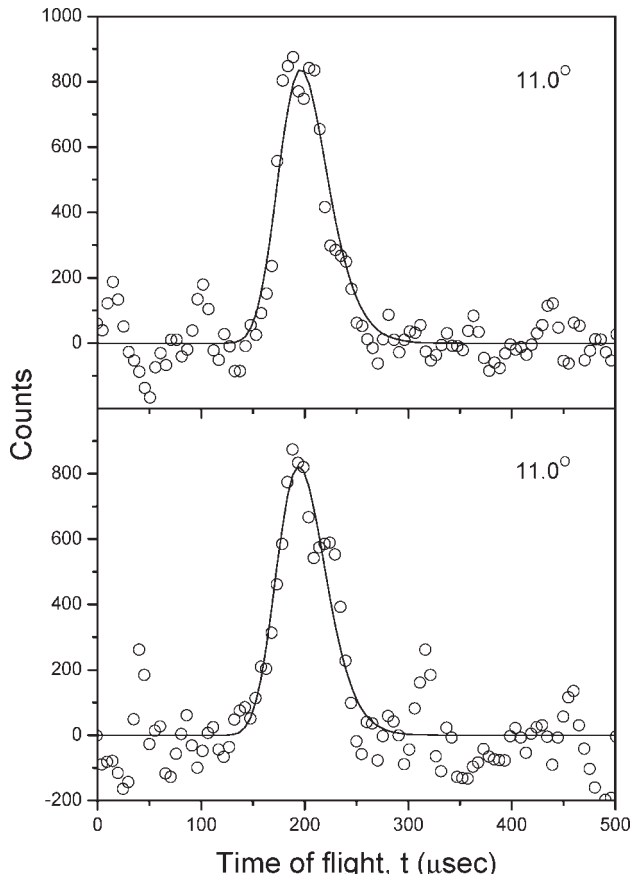


**Figure 3.** Upper: Time-of-flight spectrum recorded at the center-of-mass angle at  $m/z = 133$  ( $\text{C}_{10}\text{H}_7\text{D}_3^+$ ) during the reaction of the phenyl radical with 1,3-butadiene-1,1,4,4-D4. Lower: TOF spectrum recorded at  $m/z = 135$  ( $\text{C}_{10}\text{H}_5\text{D}_5^+$ ) in the experiment of phenyl with 1,3-butadiene-D6. The open circles are the experimental data, and the solid lines are the fits.

high-energy cutoffs, that is, the sum of the absolute energy of the reaction plus the collision energy, permit us to extract the reaction energy. By averaging over both experiments, the data suggest that the reaction is exoergic by  $48 \pm 29$   $\text{kJ mol}^{-1}$ . These data correlate nicely with the computed exoergicity, which ranges between  $42.7^{30}$  and  $30.4$   $\text{kJ mol}^{-1}$ <sup>31</sup> to form 1-phenyl-1,3-butadiene plus atomic hydrogen, channel (1e). On basis of this finding, we can extract the fraction of available energy channeled into the translational degrees of freedom of the products to be about 30.0% for both collision energies. This order of magnitude is consistent with a reaction mechanism involving complex formation.<sup>37</sup> In addition, both distributions are relatively broad and show pronounced distribution maxima in the range of  $20$ – $35$   $\text{kJ mol}^{-1}$ , that is, peaks well away from zero translational energy. As the collision energy increases, the peak position moves toward high energies. This likely indicates a tight exit transition state when the  $\text{C}_{10}\text{H}_{11}$  intermediate(s) dissociates to the final products. According to the principle of microscopic reversibility of a chemical reaction, the reverse reaction of hydrogen atom addition to the  $\text{C}_{10}\text{H}_{10}$  isomer is therefore expected to have an entrance barrier.<sup>38</sup>

The center-of-mass angular distributions help us to gain additional supporting information on the reaction dynamics. At both collision energies, the angular flux distributions show intensity over the complete angular range from  $0$  to  $180^\circ$  and are asymmetric around  $90^\circ$ , that is, an enhanced flux in the forward hemisphere with respect to the phenyl radical beam, Figure 4 (right). Note that within the error limits, the reaction

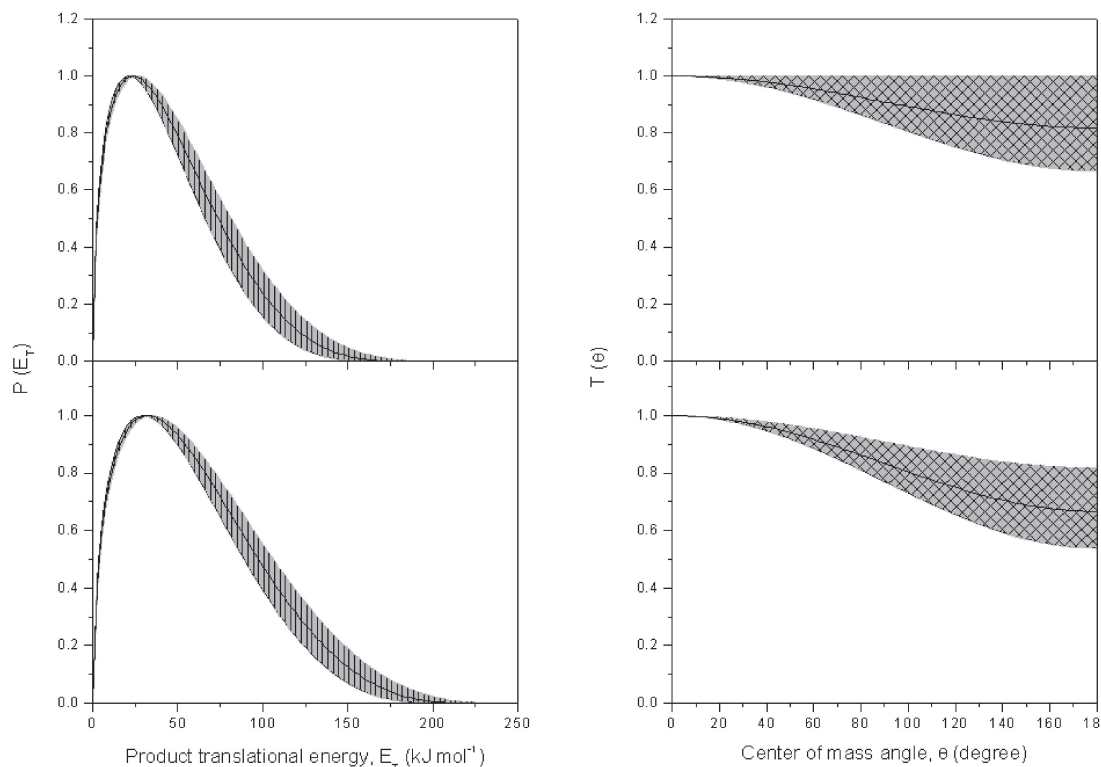


**Figure 4.** Center-of-mass translational (left) and angular (right) distribution of the  $C_{10}H_{10}$  product formed in the reaction of the phenyl radical with 1,3-butadiene at two collision energies of  $117.3 \pm 2.2$  (upper row) and  $148.7 \pm 6.3$   $\text{kJ mol}^{-1}$  (lower row). The hatched areas account for the experimental error limits of the TOF spectra (Figure 1) and the laboratory angular distribution (Figure 2); the solid lines are the best fits.

at lower collision energy could also be fit with an isotropic distribution as well. As the collision energy increases, the  $T(\theta)$ s are increasingly forward peaked. The ratios at the poles,  $I(180^\circ)/I(0^\circ)$ , changed from  $0.82 \pm 0.18$  at lower to  $0.67 \pm 0.14$  at higher collision energy. First, this suggests that the reaction follows indirect scattering dynamics via complex ( $C_{10}H_{11}$ ) formation. Second, the asymmetry of the center-of-mass angular distributions indicates that the lifetime(s) of the  $C_{10}H_{11}$  intermediate(s) is shorter than (or comparable with) its rotational period (oscillating complex) at both collision energies. Finally, as the collision energy rises, the distributions are more forward scattered; this indicates that the lifetime of the reaction intermediate(s) decreases as the collision energy rises.

#### 4. Discussion

**4.1. Product Isomer Identification.** On the basis of the recorded TOF spectra for the reaction of phenyl with 1,3-butadiene, we have demonstrated that the products are an isomer of the generic formula  $C_{10}H_{10}$  plus atomic hydrogen (channels 1d and 1e). Considering the TOF spectra observed during the  $C_6H_5 + 1,3-C_4D_6$  and  $C_6H_5 + 1,3-C_4H_2D_4$  experiments, we have shown that the emitted hydrogen atom originates solely from the terminal C1/C4 carbon atom of the 1,3-butadiene molecule. A comparison of this finding with the potential energy surface (Figure 5) reveals that the only possible channel is 1e, 1-phenyl-1,3-butadiene plus a hydrogen atom. Considering channel 1d, 1,4-dihydronaphthalene plus atomic hydrogen, the detached hydrogen atom must be released from the phenyl radical; this does not agree with the experimental results of the  $C_6H_5 + 1,3-C_4D_6$  system. Also, the center-of-mass translational energy distributions indicate that the reaction is exoergic by about  $48 \pm 29$   $\text{kJ mol}^{-1}$ . We can compare this data with theoretically computed reaction energies of possible products (Figure 5). The

energetics of the 1-phenyl-1,3-butadiene plus hydrogen atom channel (1e,  $-42.7$   $\text{kJ mol}^{-1}$ ) are in very good agreement with the experimental results. Even within the error limits, the formation of the 1,4-dihydronaphthalene isomer, which is exoergic by about  $108.8$   $\text{kJ mol}^{-1}$ , can be ruled out. We should also mention that the entrance barrier for the reverse reaction of 1-phenyl-1,3-butadiene with a hydrogen atom is about  $30.1$   $\text{kJ mol}^{-1}$ ; this order correlates nicely with the experimental data of  $20\text{--}35$   $\text{kJ mol}^{-1}$ . Hence, within the limit of our detection, the only  $C_{10}H_{10}$  isomer formed is 1-phenyl-1,3-butadiene, reaction channel 1e.

**4.2. Proposed Reaction Dynamics.** In this section, we would like to propose the most likely reaction dynamics to form the phenyl-1,3-butadiene molecule based on the experimental results as discussed above and the theoretical calculations.<sup>30,31</sup> First, we correlate the structure of the 1-phenyl-1,3-butadiene reaction product ( $C_6H_5CHCHCHCH_2$ ) with the reactants. Here, we propose that the phenyl radical adds with its radical center to the terminal carbon atoms C1/C4 (=CH<sub>2</sub> group) of the 1,3-butadiene reactant to form the 4-phenylbuten-3-yl ( $C_6H_5CH_2CHCHCH_2$ ) intermediate. This directed attack is likely influenced by two effects. First, the cone of acceptance of addition of the phenyl radical to the =CH<sub>2</sub> group of the 1,3-butadiene reactant favors the attack of the C1/C4 carbon atoms. Second, the phenyl radical must be considered as an electron-deficient reactant due to the unpaired electron. In 1,3-butadiene, the C1/C4 carbon atoms have charges of about  $-0.34$ , but the C2/C3 atom has a charge of only  $-0.27$ . Therefore, the attack is preferentially directed to the carbon atoms with the highest electron density, the terminal carbon atoms C1/C4. Also, a recent quantum chemistry computation suggested that the addition of the phenyl radical to the central carbon atoms C2/C3 has a higher entrance barrier ( $16.7$   $\text{kJ mol}^{-1}$ ) compared to a barrierless

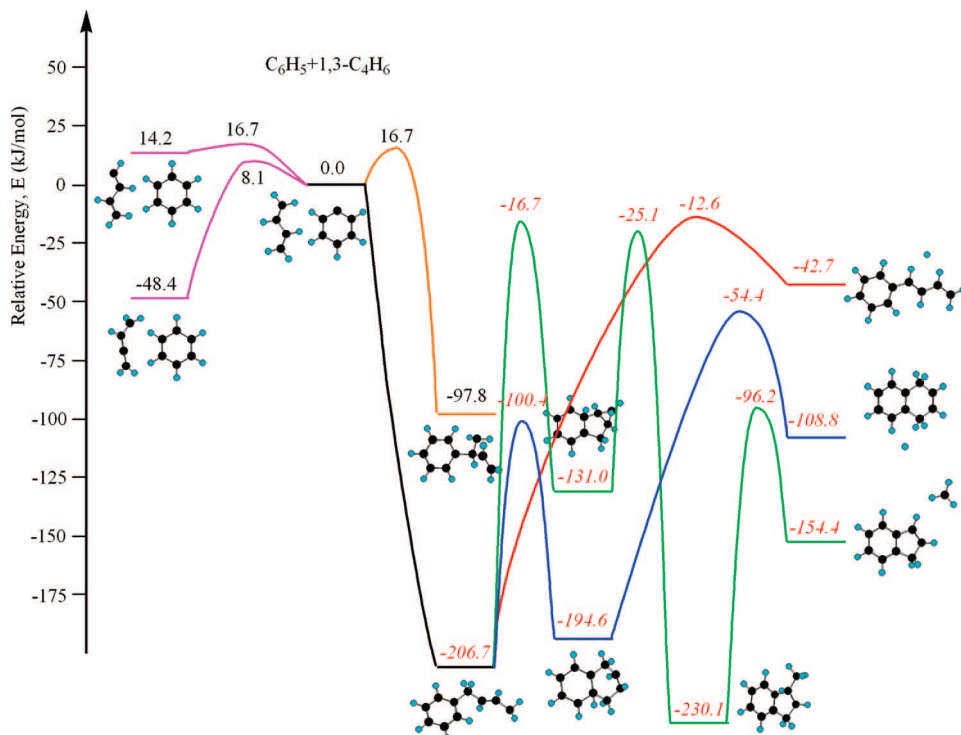


**Figure 5.** Potential energy surface for the reaction of C<sub>6</sub>H<sub>5</sub> with 1,3-butadiene. Energies in black are calculated at the B3LYP/6-31G(d,p) level of theory (ref 31); energies depicted in red are computed with G2MP2 theory (ref 30). Different reaction channels are labeled in different colors.

**TABLE 2: Moments of Inertia, Rotation Times (in ps), and Estimated Lifetimes (in ps) of the Intermediates of the Reaction of the Phenyl Radical with Unsaturated Hydrocarbons**

	rotation axis	A	B	C
C <sub>6</sub> H <sub>5</sub> + C <sub>2</sub> H <sub>4</sub> ( <i>b</i> <sub>max</sub> = 0.16 nm)	moment of inertia (10 <sup>-45</sup> kg m <sup>2</sup> )	<i>I</i> <sub>A</sub> = 1.8	<i>I</i> <sub>B</sub> = 5.6	<i>I</i> <sub>C</sub> = 6.8
	rotation period, <i>t</i> <sub>rot</sub> (ps)	<i>E</i> <sub>C</sub> = 83.6 kJ mol <sup>-1</sup>	0.7	2.3
	lifetime, <i>τ</i> (ps)	<i>E</i> <sub>C</sub> = 105.3 kJ mol <sup>-1</sup>	0.6	2.0
C <sub>6</sub> H <sub>5</sub> + H <sub>2</sub> CCCH <sub>2</sub> ( <i>b</i> <sub>max</sub> = 0.23 nm)	moment of inertia (10 <sup>-45</sup> kg m <sup>2</sup> )	<i>I</i> <sub>A</sub> = 2.5	<i>I</i> <sub>B</sub> = 7.6	<i>I</i> <sub>C</sub> = 8.1
	rotation period, <i>t</i> <sub>rot</sub> (ps)	<i>E</i> <sub>C</sub> = 92.7 kJ mol <sup>-1</sup>	0.6	1.8
	lifetime, <i>τ</i> (ps)	<i>E</i> <sub>C</sub> = 117.4 kJ mol <sup>-1</sup>	0.5	1.6
C <sub>6</sub> H <sub>5</sub> + C <sub>3</sub> H <sub>6</sub> ( <i>b</i> <sub>max</sub> = 0.23 nm)	moment of inertia (10 <sup>-45</sup> kg m <sup>2</sup> )	<i>I</i> <sub>A</sub> = 2.4	<i>I</i> <sub>B</sub> = 8.1	<i>I</i> <sub>C</sub> = 9.3
	rotation period, <i>t</i> <sub>rot</sub> (ps)	<i>E</i> <sub>C</sub> = 130.2 kJ mol <sup>-1</sup>	0.5	1.6
	lifetime, <i>τ</i> (ps)	<i>E</i> <sub>C</sub> = 130.2 kJ mol <sup>-1</sup>	0.3	1.1
C <sub>6</sub> H <sub>5</sub> + 1,3-C <sub>4</sub> H <sub>6</sub> ( <i>b</i> <sub>max</sub> = 0.32 nm)	moment of inertia (10 <sup>-45</sup> kg m <sup>2</sup> )	<i>I</i> <sub>A</sub> = 2.7	<i>I</i> <sub>B</sub> = 12.5	<i>I</i> <sub>C</sub> = 13.5
	rotation period, <i>t</i> <sub>rot</sub> (ps)	<i>E</i> <sub>C</sub> = 117.3 kJ mol <sup>-1</sup>	0.4	1.7
	lifetime, <i>τ</i> (ps)	<i>E</i> <sub>C</sub> = 148.7 kJ mol <sup>-1</sup>	0.3	1.5

addition to the terminal carbon atoms C1/C4.<sup>30,31</sup> Consequently, the sterical effect, the enhanced negative charge density, and the lower entrance barrier (even if our collision energies are higher than the computed barrier) likely direct the addition of the phenyl radical to the terminal carbon atom of 1,3-butadiene. A similar directed addition of the phenyl radical to the less substituted carbon atom has been observed in the reaction with methylacetylene (CH<sub>3</sub>CCH),<sup>12</sup> allene (H<sub>2</sub>CCCH<sub>2</sub>),<sup>12</sup> and propylene (CH<sub>3</sub>CHCH<sub>2</sub>).<sup>13</sup> To summarize, the addition of the phenyl radical to the terminal carbon atom leads to the formation of a 4-phenylbuten-3-yl (C<sub>10</sub>H<sub>11</sub>) reaction intermediate. These complex formation reaction dynamics have also been inferred from the center-of-mass angular distributions. This intermediate can undergo unimolecular decomposition via atomic hydrogen

detachment involving a tight exit transition state. The computations suggested that the transition state resides 30.1 kJ mol<sup>-1</sup> above the separate products; the existence of an exit barrier has been verified by experimental results of the off-zero peaking (20–35 kJ mol<sup>-1</sup>) of the center-of-mass translational energy distribution.

It is very important to address the failed detection of the energetically favorable 1,4-dihydronaphthalene isomer (1d). This channel would require an isomerization to form a bicyclic intermediate (1,4,9-trihydronaphthalene) followed by a detachment of atomic hydrogen originating from the phenyl radical to form the products. This process demands more time to overcome one additional transition state to ring closure; as for the 1,4,9-trihydronaphthalene intermediate, the most favorable

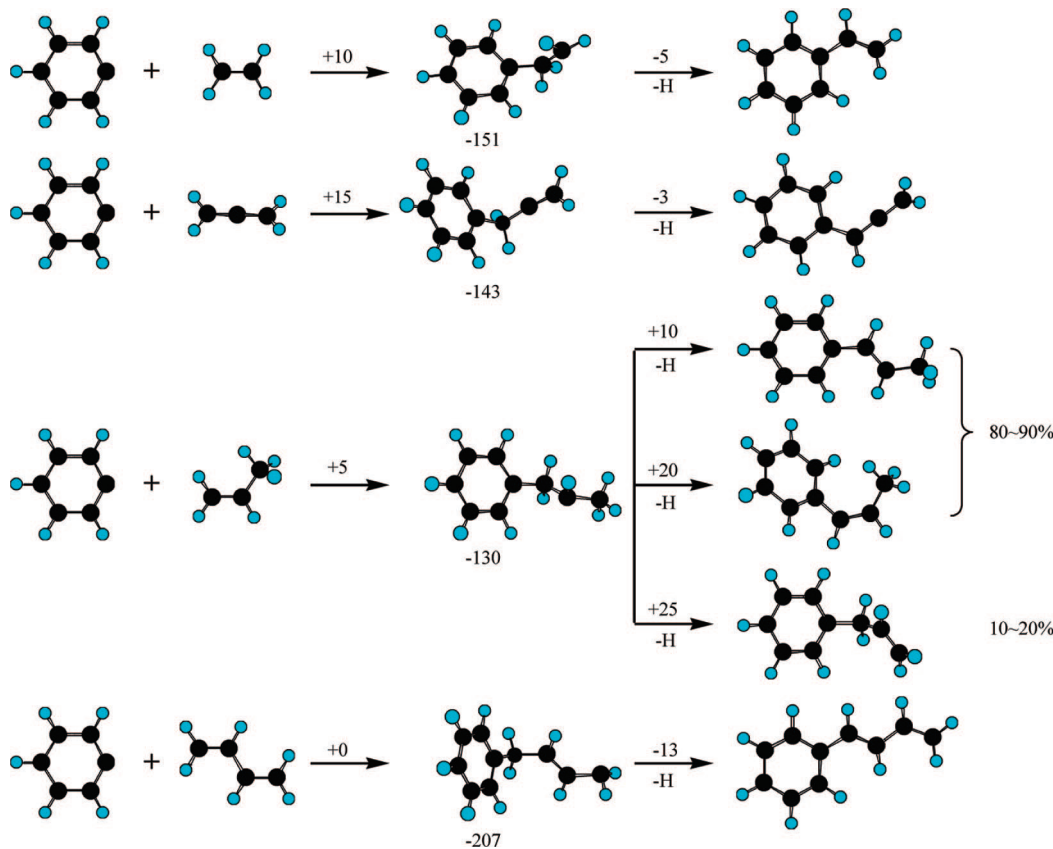


**Figure 6.** Schematic representations of the reactions of the phenyl radical with unsaturated hydrocarbons containing double bonds. Energies are given in  $\text{kJ mol}^{-1}$ .

channel is isomerization back to 4-phenylbuten-3-yl. This can explain the failed detection of the isomer 1,4-dihydronaphthalene; the lifetime of the initial addition complex is too short to allow an isomerization via cyclization to 1,4,9-trihydronaphthalene. We also have to discuss the failed detection of the methyl group loss (1f). This mechanism requires an isomerization of the initial adduct via a significant barrier ( $190.0 \text{ kJ mol}^{-1}$ ) to form a cyclopentadienyl derivative. The latter would undergo an isomerization to yield a stable methylcyclopentenyl-type radical via hydrogen atom transfer from the phenyl radical to the  $\text{CH}_2$  group and a simultaneous C–C bond rupture. Again, on the basis of our results, the formation of the cyclopentadienyl-type intermediate is likely blocked by the inherent barrier to isomerization, and a hydrogen atom emission from the initial collision complex is more likely.

Finally, the collision energy dependence of the reaction dynamics should be mentioned. From the center-of-mass angular distributions, the enhanced forward scattering with increasing collision energy is evident. We have elucidated the 4-phenylbuten-3-yl as the sole intermediate to form 1-phenyl-1,3-butadiene. Here, we attempt to estimate the lifetime of this intermediate at different collision energy. Recall that the intermediate can be treated as an osculating complex. The rotational period ( $t_{\text{rot}}$ ) of this intermediate serves as a clock in the crossed molecular beam experiments and can be utilized to evaluate the lifetime ( $\tau$ ) of the decomposing complex. The osculating complex model connects the lifetime  $\tau$  with the intensity ratio at the poles ( $I(180^\circ)/I(0^\circ)$ ) via eq 4.<sup>39</sup> Here,  $L_{\text{max}}$  represents the maximum orbital angular momentum of the reaction, which can be approximated from the maximum impact parameter ( $b_{\text{max}}$ ), relative velocity ( $v_{\text{rel}}$ ), and reduced mass ( $\mu$ ) of the reactants.  $I_i$  stands for the moment of inertia of the complex rotating around the  $i$  axis ( $i = A, B, C$ ).

$$t_{\text{rot}} = \frac{2\pi I_i}{L_{\text{max}}} = \frac{2\pi I_i}{\mu \times b_{\text{max}} \times v_{\text{rel}}} \quad (i = A, B, C) \quad (4)$$

$$\tau = \frac{-t_{\text{rot}}}{2 \ln(I(180^\circ)/I(0^\circ))}$$

Using the ab initio geometries of the intermediates from refs 30 and 31, we can determine the moments of inertia and the maximum impact parameter ( $\sim 0.32 \text{ nm}$ ). This yields the maximum orbital angular momenta ( $L_{\text{max}}$ ) of  $46 \times 10^{-33} \text{ kg m}^2 \text{ s}^{-1}$  for a collision energy of  $117.3 \text{ kJ mol}^{-1}$  and  $52 \times 10^{-33} \text{ kg m}^2 \text{ s}^{-1}$  for  $148.7 \text{ kJ mol}^{-1}$ . The lifetimes  $\tau$  of the intermediates depend on the rotation axis and are compiled in Table 2. Even at the higher collision energy,  $E_C = 148.7 \text{ kJ mol}^{-1}$ , we can conclude that the lifetime of the complex is longer than its rotational period,  $t_{\text{rot}}$ , and on the order of  $0.4\text{--}4.5 \text{ ps}$ . On the basis of the experiments, these lifetimes are still too short to allow the initial collision complex to rearrange to other  $C_{10}H_{11}$  isomers (recall that we did not detect the 1,4-dihydronaphthalene and indene products). Considering the reactions of phenyl with ethylene, allene, and propylene, it is clear that at a similar collision energy, the lifetime of the decomposing intermediate is enhanced as the number of atoms and hence vibrational modes increase.

**4.3. Comparison with Other Reactions of the Phenyl Radical with Unsaturated Hydrocarbons with Double Bonds.** It is meaningful to compare the reaction dynamics of the phenyl radical plus 1,3-butadiene with those of the phenyl radical with ethylene,<sup>11</sup> allene,<sup>12</sup> and propylene<sup>13</sup> investigated earlier in our group. At all collision energies from  $83.6$  to  $148.7 \text{ kJ mol}^{-1}$ , the TOF spectra can be fitted with only one hydrogen atom substitution channel. The LABORATORY distributions of the heavy products are very narrow and spread over only about  $10\text{--}14^\circ$ . All center-of-mass angular distributions are asymmetric

and show intensity over the complete angular range from 0 to 180° and enhanced flux in the forward hemisphere. These data suggest that all reactions follow indirect scattering dynamics via oscillating complexes (C<sub>8</sub>H<sub>9</sub>, C<sub>9</sub>H<sub>9</sub>, C<sub>9</sub>H<sub>11</sub>, C<sub>10</sub>H<sub>11</sub>). All product translational energy distributions,  $P(E_T)$ , show distribution maxima away from zero translational energy, which suggests that these reactions involve tight exit transition states. Using fully deuterated isotopologues (C<sub>2</sub>D<sub>4</sub>, C<sub>3</sub>D<sub>4</sub>, C<sub>3</sub>D<sub>6</sub>, C<sub>4</sub>D<sub>6</sub>), we found that the detached atoms are solely from the unsaturated hydrocarbon molecules; the phenyl radicals are likely to be conserved in the reactions (Figure 6). The phenyl radical always adds its radical center to the terminal carbon atom with double bond (=CH<sub>2</sub> group) to form the intermediate; as mentioned above, this is mainly due to sterical and electron density effects. The dominant products are styrene, 1-phenylallene, *cis/trans*-1-phenylpropene (80–90%), and 1-phenyl-1,3-butadiene. The lifetimes of the decomposition intermediates increase with the number of atoms of the scattering system from 0.1 up to 4.5 ps. However, it is evident that this increase in lifetime is still not sufficient to allow ring closure processes. Recall that the supersonic phenyl beam is generated via flash pyrolysis of nitrosobenzene. The velocity of the beam is about 2500–3500 ms<sup>-1</sup>; if we can reduce the velocity of the phenyl radical beam and hence the collision energy, this should result in an enhanced lifetime of the intermediate. This cannot be done by simply changing the carrier gas to heavier species such as neon or argon; these atoms are relatively inefficient to quantitatively cleave the carbon–nitrogen bond in the nitrosobenzene molecule. Likewise, the residence time of the phenyl radicals in the silicon carbide tube would be enhanced, thus favoring dimerization to form the diphenyl molecule. However, photolytically generated phenyl radical can have lower velocities. This might allow an isomerization via ring closure and hence the formation of bicyclic, aromatic structures.

## 5. Conclusions and Summary

In our laboratory, the reactions of the phenyl radical with 1,3-butadiene together with its deuterated counterparts (1,3-butadiene-D6, 1,3-butadiene-1,1,4,4-D4) were investigated under single-collision conditions utilizing a crossed molecular beams machine. The chemical dynamics extracted from the experimental data proposed that this reaction is indirect and through an oscillating complex intermediate. It is initiated by an addition of the phenyl radical to the terminal carbon atom C1/C4 of the 1,3-butadiene molecule, that is, at the =CH<sub>2</sub> unit without an entrance barrier. This leads to the formation of a radical intermediate (4-phenylbuten-3-yl). The latter decomposes through a tight exit transition state to yield the 1-phenyl-1,3-butadiene plus atomic hydrogen. The overall reaction was found to be exoergic by 48 ± 29 kJ mol<sup>-1</sup>. Our experimental investigation provides sturdy evidence that precursors to PAHs can be formed in combustion flames and in the circumstellar envelopes of carbon-rich stars such as IRC+10126 and planetary nebulae like CRL 618<sup>40</sup> via phenyl radical reactions, here, with 1,3-butadiene, where temperatures of up to a few 1000 K reside.

**Acknowledgment.** This work was supported by the U.S. Department of Energy, Basic Energy Sciences (DE-FG02-03ER15411). We would also like to thank Ed Kawamura (University of Hawaii, Department of Chemistry) for assistance.

## References and Notes

- (1) Kunzli, N.; Kaiser, R.; Medina, S.; Studnicka, M.; Chanel, O.; Filliger, P.; Herry, M.; Horak, F.; Puybonnieux-Texier, V.; Quenel, P.; Schneider, J.; Seethaler, R.; Vergnaud, J. C.; Sommer, H. *Lancet* **2000**, 356, 795.
- (2) Denissenko, M. F.; Pao, A.; Tang, M.-S.; Pfeifer, G. P. *Science* **1996**, 274, 430.
- (3) Durant, J. L.; Busby, W. F.; Lafleur, A. L.; Penman, B. W.; Crespi, C. L. *Mutat. Res.* **1996**, 371, 123.
- (4) Cox, P., Kessler, M. F., Eds. *The Universe as Seen by ISO, ESA, SP-427*; European Space Agency: Noordwijk, The Netherlands, 1999; Vol. II.
- (5) Allamandola, L. J.; Hudgins, D. M.; Sandford, S. A. *Astrophys. J. Lett.* **1999**, 511, L115.
- (6) Dwek, E.; Arendt, R. G.; Fixsen, D. J.; Sodroski, T. J.; Odegard, N.; Weiland, J. L.; Reach, W. T.; Hauser, M. G.; Kelsall, T.; Moseley, S. H.; Silverberg, R. F.; Shafer, R. A.; Ballester, J.; Bazell, D.; Isaacman, R. *Astrophys. J. Lett.* **1997**, 475, 565.
- (7) Hausmann, M.; Homann, K. H. *Radical Analysis in Flames by Scavenging with Dimethyl Disulfide*; 22nd International Annual Conference of ICT (Combust. React. Kinet.), 1991; 22/1–12.
- (8) Law, M. E.; Westmoreland, P. R.; Cool, T. A.; Wang, J.; Hansen, N.; Taatjes, C. A.; Kasper, T. *Proc. Combust. Inst.* **2007**, 31, 565.
- (9) Park, J.; Tokmakov, I. V.; Lin, M. C. *J. Phys. Chem. A* **2007**, 111, 6881–6889.
- (10) Gu, X.; Zhang, F.; Guo, Y.; Kaiser, R. I. *Angew. Chem., Int. Ed.* **2007**, 46, 6866.
- (11) Zhang, F.; Gu, X.; Guo, Y.; Kaiser, R. I. *J. Org. Chem.* **2007**, 72, 7597.
- (12) Gu, X.; Zhang, F.; Guo, Y.; Kaiser, R. I. *J. Phys. Chem. A* **2007**, 111, 11450.
- (13) Zhang, F.; Gu, X.; Guo, Y.; Kaiser, R. I. *J. Phys. Chem. A* **2008**, 112, 3284.
- (14) Zhang, F.; Gu, X.; Kaiser, R. I. *J. Chem. Phys.* **2008**, 128, 084315/1–084315/5.
- (15) Gu, X.; Guo, Y.; Zhang, F.; Mebel, A. M.; Kaiser, R. I. *Faraday Discuss.* **2006**, 133, 245.
- (16) Bockhorn, H. *Soot Formation in Combustion: Mechanisms and Models*; Springer: Berlin, Germany, 1994.
- (17) Richter, H.; Howard, J. B. *Prog. Energy Combust. Sci.* **2000**, 26, 565.
- (18) Cole, J. A.; Bittner, J. D.; Longwell, J. P.; Howard, J. B. *Combust. Flame* **1984**, 56, 51.
- (19) Lindstedt, R. P.; Skevis, G. *Benzene Formation Chemistry in Premixed 1,3-Butadiene Flames*, 26th Symposium (International) on Combustion, The Combustion Institute, 1996; pp 703–709.
- (20) Phillip, R. W.; Anthony, M. D.; Jack, B. H.; John, P. L. *J. Phys. Chem.* **1989**, 93, 8171.
- (21) Laskin, A.; Wang, H.; Law, C. K. *Int. J. Chem. Kinet.* **2000**, 32, 589.
- (22) Granata, S.; Faravelli, T.; Ranzi, E.; Olten, N.; Senkan, S. *Combust. Flame* **2002**, 131, 273.
- (23) Olten, N.; Senkan, S. *Combust. Flame* **2001**, 125, 1032.
- (24) Frenklach, M.; Clary, D. W.; Gardiner, W. C.; Stein, S. E. *Effect of Fuel Structure on Pathways to Soot*; 21st Symposium (International) on Combustion, The Combustion Institute: Pittsburgh, PA, 1986; Vol. 1067, p 76.
- (25) Chambreau, S. D.; Lemieux, J.; Wang, L.; Zhang, J. *J. Phys. Chem. A* **2005**, 109, 2190.
- (26) Hidaka, Y.; Higashihara, T.; Ninomiya, N.; Masaoka, H.; Nakamura, T.; Kawano, H. *Int. J. Chem. Kinet.* **1996**, 28, 137.
- (27) (a) Kiefer, J. H.; Wei, H. C.; Kern, R. D.; Wu, C. H. *Int. J. Chem. Kinet.* **1985**, 17, 225. (b) Kiefer, J. H.; Mitchell, K. I.; Wei, H. C. *Int. J. Chem. Kinet.* **1988**, 20, 787. (c) Benson, S. W.; Haugen, G. R. *J. Phys. Chem.* **1967**, 71, 1735.
- (28) (a) Wu, C. H.; Kern, R. D. *J. Phys. Chem.* **1987**, 91, 6291. (b) Kern, R. D.; Singh, H. J.; Wu, C. H. *Int. J. Chem. Kinet.* **1988**, 20, 731. (c) Hidaka, Y.; Higashihara, T.; Ninomiya, N.; Oki, T.; Kawano, H. *Int. J. Chem. Kinet.* **1995**, 27, 331.
- (29) (a) Skinner, G. B.; Sokolowski, E. M. *J. Phys. Chem.* **1960**, 64, 1028. (b) Rao, V. S.; Takeda, K.; Skinner, G. B. *Int. J. Chem. Kinet.* **1988**, 20, 153.
- (30) Fascella, S.; Cavallotti, C.; Rota, R.; Carra, S. *J. Phys. Chem. A* **2004**, 108, 3829.
- (31) Ismail, H.; Park, J.; Wong, B. M., Jr.; Lin, M. C. *Proc. Combust. Inst.* **2005**, 30, 1049.
- (32) Stranges, D.; Stemmler, M.; Yang, X.; Chesko, J. D.; Suits, A. G.; Lee, Y. T. *J. Chem. Phys.* **1998**, 109, 5372.
- (33) Kohn, D. W.; Clauberg, H.; Chen, P. *Rev. Sci. Instrum.* **1992**, 63, 4003.
- (34) Kaiser, R. I.; Asvany, O.; Lee, Y. T.; Bettinger, H. F.; Schleyer, P. v. R.; Schaefer, H. F., III. *J. Chem. Phys.* **2000**, 112, 4994.
- (35) (a) Kaiser, R. I.; Le, T. N.; Nguyen, T. L.; Mebel, A. M.; Balucani, N.; Lee, Y. T.; Stahl, F.; Schleyer, P. v. R.; Schaefer, H. F., III. *Faraday Discuss.* **2001**, 119, 51. (b) Vernon, M. Ph.D. Thesis, University of California, Berkley, CA, 1981. (c) Weiss, M. S. Ph.D. Thesis, University of California, Berkley, CA, 1986.

- (36) Levine, R. D. *Molecular Reaction Dynamics*; Cambridge University Press: Cambridge, U.K., 2005.
- (37) Kaiser, R. I.; Mebel, A. M. *Int. Rev. Phys. Chem.* **2002**, *21*, 307.
- (38) Steinfeld, J. I.; Francisco, J. S.; Hase, W. L. *Chemical Kinetics and Dynamics*; Prentice Hall: Upper Saddle River, NJ, 1999.
- (39) Miller, W. B.; Safron, S. A.; Herschbach, D. R. *Discuss. Faraday Soc.* **1967**, *44*, 108.
- (40) Cernicharo, J.; Heras, A. M.; Tielens, A.; G, G. M.; Pardo, J. R.; Herpin, F.; Guelin, M.; Waters, L. B. F. M. *Astrophys. J. Lett.* **2001**, *546*, L123.  
JP809364V